Available online at www.sciencedirect.com
SCIENCE DIRECT®
Chemical Physics 301 (2004) 293–308
Chemical Physics
www.elsevier.com/locate/chemphys

Sign of the state-to-state steric asymmetry of rotationally inelastic atom–molecule collisions

A. Gijsbertsen [a], M.J.L. de Lange [a,1], A.E. Wiskerke [a], H. Linnartz [a], M. Drabbels [b], J. Kłos [c], S. Stolte [a,*]

[a] *Laser Centre and Department of Physical Chemistry, Faculty of Exact Sciences, Vrije Universiteit Amsterdam, De Boelelaan 1083, 1081 HV Amsterdam, The Netherlands*
[b] *Institute of Molecular and Biological Chemistry, Swiss Federal Institute of Technology Lausanne (EPFL), 1015 Lausanne, Switzerland*
[c] *Institute of Theoretical Chemistry, University of Nijmegen, Toernooiveld 1, 6525 ED Nijmegen, The Netherlands*

Received 6 November 2003; accepted 5 February 2004
Available online 2 April 2004

Abstract

The sign of the theoretically predicted steric asymmetry S in rotational inelastic state resolved molecule–atom collisions is questioned. It is shown that the sign of the T-matrix obtained on a basis of non-oriented rotational states of the molecule depends on the choice of the Jacobi coordinates in which the collision problem is solved. Explicit expressions for the state-to-state dependence of the integral and differential cross-sections for oriented and non-oriented molecules are presented. The effect of the choice of Jacobi angles and the inertial frame of reference on the sign of S are discussed in detail. The sign of the earliest obtained expression for the steric asymmetry of the integral cross-section (as reported by van Leuken et al.) is found to be correct, whereas that of the orientational-dependent contribution of the differential cross-section (as reported by Alexander and Stolte) requires a negative multiplication factor. Quantum mechanical calculations on collisions of OH with Ar are performed. These calculations do not agree with the experimental sign of S and cannot be interpreted in terms of a simple ball and stick model. Inspection of the HIBRIDON source code shows that the prepared wavefunction carries an orientation that is opposite to the one assumed. This could offer an explanation for the disagreement for S. For collisions of NO with Ar, the signs of the quantum mechanically calculated and the experimental values of S appear to disagree with the simple ball and stick model. The experimental sign of S has been reinvestigated. Previous experimental results are confirmed.

1. Introduction

Orientation effects in atom–molecule collisions are commonly described using the steric asymmetry S, that is defined as

$$S = \frac{\sigma^{\mathrm{Head}} - \sigma^{\mathrm{Tail}}}{\sigma^{\mathrm{Head}} + \sigma^{\mathrm{Tail}}}. \tag{1}$$

Here σ^{Head} and σ^{Tail} denote the cross-sections for molecules oriented preferentially with their head or tail towards the atom. The first striking experimental evidence for large orientation effects in rotationally inelastic state-resolved NO (ON) and Ar collisions, was performed by van Leuken et al. [1]. In their convention, the N-end and the O-end of the NO molecule were defined as head and tail, respectively. In addition, quantum mechanical scattering calculations were performed. Van Leuken and coworkers succeeded in deriving a contracted equation that expresses the difference between the integral cross-sections for N-end preferred and O-end preferred collisions (respectively, $\sigma^{\mathrm{NO}}_{j,m_j,\overline{\Omega},E\to j',m'_j,\overline{\Omega}',\epsilon'}$

* Corresponding author. Fax: +31-20-444-7643.
E-mail address: stolte@few.vu.nl (S. Stolte).
[1] Present address: Molecular Cytology, Swammerdam Institute for Life Sciences, University of Amsterdam, P.O. Box 94062, 1090 GB Amsterdam, The Netherlands.

0301-0104/$ - see front matter © 2004 Elsevier B.V. All rights reserved.
doi:10.1016/j.chemphys.2004.02.003

and $\sigma^{\mathrm{ON}}_{j,m_j,\overline{\Omega},E\to j',m'_j,\overline{\Omega}',\epsilon'}$) into a weighted sum over products of T-matrix elements. The total angular momentum of a diatomic (or a symmetric top alike) molecule is denoted by j, having projections Ω and m_j along, respectively, the molecular axis and the space-fixed Z-axis. The absolute value of Ω is written as $\overline{\Omega}$ and ϵ $(=-1,1)$ gives the symmetry index that distinguishes between the two components of the Λ-doublet [2]. The index E indicates the electric orientation field at the scattering region.

In NO–Ar collisions the O-end was reported to be preferred for high rotational final states [1,3–5]. This is not what one would expect from a simple ball and stick model that seems to apply very well in OH–Ar collisions [6]: the O-end is more round (ball) than the H-end (stick) that extends further from the center-of-mass (CM) of the OH molecule. As a consequence, high rotational final states prefer H-end collisions.

This paper focusses on the sign of the steric asymmetry. It is organized in the following way. Section 2 consists of a number of relevant experimental and theoretical considerations. In Section 3, the sign issue concerning the steric asymmetry is introduced. Experimental results for collisions of OH with Ar serve as a benchmark system here, as experimentally observed rotational state transitions exhibit a propensity in S that can qualitatively be understood in a simple ball and stick model. These experimental results for S are compared to those obtained from new close coupling calculations (HIBRIDON [7]) that have been carried out on the most recent UMP4 ab initio PESs for OH–Ar, developed by Kłos et al. [8]. Section 4 focusses on the parameters that are involved in defining the sign of the steric effect. We will show that the T-transition matrix that results from HIBRIDON, $T^J_{j',l',\overline{\Omega}',\epsilon';j,l,\overline{\Omega},\epsilon}$, depends on the choice of Jacobi coordinates that parameterize the interaction PESs. The resulting scattering amplitude depends also on the actual choice of the inertial coordinate frame of the corresponding center-of-mass system (CMS). The cases of the space fixed Z-axis parallel and anti-parallel to the incoming relative velocity vector are considered.

If one chooses the Jacobi coordinates such that the displacement vector **R** points from the atom to the molecule, the relative velocity vector points oppositely to the conventional case in which **R** points from the molecule to the atom. The outcome for the T-matrix will depend upon this choice of **R**. This dependence is typically unimportant in cases other than those in which steric effects are concerned. In Section 5, an experimental investigation is reported that confirms the sign and magnitude of S that was found in earlier experiments. In Section 6, we will close with a brief discussion and concluding remarks.

2. Experimental and theoretical considerations

To be experimentally observable, the determination of the steric asymmetry requires the application of a homogeneous electric orientation field **E** in a direction parallel or anti-parallel to the relative velocity vector of the colliding particles. The NO-beam can be state selected in the upper component (u) of the Λ-doublet ($^2\Pi_{1/2}$, $j=\frac{1}{2}$, $\epsilon=\epsilon_{\mathrm{u}}=-1$) by hexapole focussing. All focussed molecules reside in a low field seeking state for which $m_j=+\overline{m}_j$ and $m_j=-\overline{m}_j$ have equal probability. Having applied **E** at the scattering volume, either the O-end (tail) or the N-end (head) predominantly points towards the incoming Ar atom. The field strength is chosen such ($E\approx 16$ kV/cm) that it is sufficiently large to mix the selected $|j,m_j,\overline{\Omega},\epsilon_{\mathrm{u}}\rangle$ and the $|j,m_j,\overline{\Omega},-\epsilon_{\mathrm{u}}\rangle$ components of the Λ-doublet of opposite parity with (positive) mixing coefficients $\alpha(E)$ and $\beta(E)$. The oriented wavefunction as follows as

$$\big|j,m_j,\overline{\Omega},E\big\rangle=\alpha(E)\big|j,m_j,\overline{\Omega},\epsilon_{\mathrm{u}}\big\rangle\pm\beta(E)\big|j,m_j,\overline{\Omega},-\epsilon_{\mathrm{u}}\big\rangle, \tag{2}$$

with $\alpha(E)^2+\beta(E)^2=1$ [9]. Note that this convention deviates from that of [4] in which the role of α and β is reversed and their absolute value is multiplied by $\sqrt{2}$. Because one has to do with a low field seeking state, $\alpha(E)>\beta(E)\geqslant 0$. The $\pm$ denotes which molecular end is preferred to point along **E**. Neglecting Hund case b mixing for the moment, the rotational wavefunction can, for arbitrary values of ϵ, be written as [10]

$$\big|j,m_j,\overline{\Omega},\epsilon\big\rangle\equiv\frac{1}{\sqrt{2}}\left[\big|j,m_j,+\overline{\Omega}\big\rangle+\epsilon\big|j,m_j,-\overline{\Omega}\big\rangle\right]. \tag{3}$$

Besides large enough for mixing, we assume E to remain small enough to keep the Stark shift of the spacing between the rotational energy levels minor. Test calculations showed that these shifts (in the order of Λ-doublet splitting) had negligible effect on the calculated cross-sections [1]. As the energy may be assumed independent of the actual values of $\alpha(E)$ and $\beta(E)$, van Leuken et al. [1] expressed the T-matrix elements for an incoming oriented rotational state $|j,m_j,\overline{\Omega},E\rangle$ and non-oriented outgoing state $|j',m'_j,\overline{\Omega'},\epsilon'\rangle$ as

$$T_{j',m'_j,l',m'_l,\overline{\Omega}',\epsilon';j,m_j,l,m_l,\overline{\Omega},E}=\alpha(E)T_{j',m'_j,l',m'_l,\overline{\Omega}',\epsilon';j,m_j,l,m_l,\overline{\Omega},\epsilon_{\mathrm{u}}}\ \pm\ \beta(E)T_{j',m'_j,l',m'_l,\overline{\Omega}',\epsilon';j,m_j,l,m_l,\overline{\Omega},-\epsilon_{\mathrm{u}}}. \tag{4}$$

The orbital angular momentum of the incoming and outgoing state are, respectively, represented by the quantum numbers l and l', with projections m_l and m'_l on the Z-axis. The uncoupled representation of the T-matrix

$T_{j',m'_j,l',m'_l,\overline{\Omega}',\epsilon';j,m_j,l,m_l,\overline{\Omega},\epsilon}$, where the T-matrix relates to the scattering S-matrix as $\mathbf{T} = \mathbf{1} - \mathbf{S}$, assumes incoming and outgoing waves with a single direction of the space fixed quantization axis. The uncoupled representation of the T-matrix relates to the coupled representation as

$$T_{j',m'_j,l',m'_l,\overline{\Omega}',\epsilon';j,m_j,l,m_l,\overline{\Omega},\epsilon} = \sum_{J,M_J} T^J_{j',l',\overline{\Omega}',\epsilon';j,l,\overline{\Omega},\epsilon} \langle J\ M_J\ |j'\ m'_j\ l'\ m'_l\rangle\ \langle J\ M_J\ |j\ m_j\ l\ m_l\rangle. \tag{5}$$

The coupled T-matrix $T^J_{j',l',\overline{\Omega}',\epsilon';j,l,\overline{\Omega},\epsilon}$ is independent of $M = m_j + m_l = m'_j + m'_l$ and diagonal in J [11]. Unlike Alexander, who uses $T^J_{j',l',\overline{\Omega}',\epsilon';j,l,\overline{\Omega},\epsilon}$ [12], van Leuken et al. use the coupled representation $T^J_{l',j',\overline{\Omega}',\epsilon';l,j,\overline{\Omega},\epsilon}$ [1]. Some algebra with Wigner 3j symbols leads to the straightforward relation between Alexander's and van Leuken et al. coupled representations as

$$T^J_{j',l',\overline{\Omega}',\epsilon';j,l,\overline{\Omega},\epsilon} = (-1)^{l'+l+j'+j+2J} T^J_{l',j',\overline{\Omega}',\epsilon';l,j,\overline{\Omega},\epsilon}. \tag{6}$$

Alexander relates the T-matrix expression of Eq. (5) to the dimensionless scattering amplitude for a transition between two states [4]

$$\begin{aligned} f_{j,m_j,\overline{\Omega},\epsilon\to j',m'_j,\overline{\Omega}',\epsilon'}(\hat{\mathbf{k}}') = \sqrt{\pi}\sum_{J,l,l'}(2l+1)^{1/2}(2J+1) i^{l-l'} \begin{pmatrix} j & J & l \\ m_j & -m_j & 0 \end{pmatrix} \\ \times \begin{pmatrix} j' & J & l' \\ m'_j & -m_j & m_j - m'_j \end{pmatrix} Y_{l',m_j-m'_j}(\hat{\mathbf{k}}') T^J_{j',l',\overline{\Omega}',\epsilon';j,l,\overline{\Omega},\epsilon} \end{aligned} \tag{7}$$

where $(:::)$ is a Wigner 3j-symbol [10]. The sum extends over all allowed values of the initial and final orbital angular momenta l and l'. The initial and final wave vectors are denoted by $\mathbf{k}$ and $\mathbf{k}'$. The direction of the initial velocity vector $\hat{\mathbf{k}}$, defines the axis of m_j quantization in the so-called "collision frame". Combination of Eqs. (4) and (7) gives

$$f_{j,m_j,\overline{\Omega},E\to j',m'_j,\overline{\Omega}',\epsilon'}(\hat{\mathbf{k}}') = \alpha(E) f_{j,m_j,\overline{\Omega},\epsilon_u;j',m'_j,\overline{\Omega}',\epsilon'} \pm \beta(E) f_{j,m_j,\overline{\Omega},-\epsilon_u;j',m'_j,\overline{\Omega}',\epsilon'}. \tag{8}$$

Eq. (8) relates directly to the differential scattering cross-section of an oriented molecule [4]:

$$\mathrm{d}\sigma_{j,m_j,\overline{\Omega},E\to j',m'_j,\overline{\Omega}',\epsilon'}/\mathrm{d}\omega = \frac{1}{k^2}\left| f_{j,m_j,\overline{\Omega},E\to j',m'_j,\overline{\Omega}',\epsilon'}(\hat{\mathbf{k}}')\right|^2. \tag{9}$$

Integration of the differential cross-section $\mathrm{d}\sigma_{j,m_j,\overline{\Omega},E\to j',m'_j,\overline{\Omega}',\epsilon'}/\mathrm{d}\omega$ in Eq. (9) over all scattering angles, provides the integral scattering cross-section $\sigma_{j,m_j,\overline{\Omega},E\to j',m'_j,\overline{\Omega}',\epsilon'}$. Using the scattering amplitude instead of the T-matrix for the treatment of molecular orientation offers a more direct insight into the underlying collision properties, leading to a better understanding of the origin and magnitude of the observed steric effects [1,5–6,13–17].

3. Considerations regarding the sign of the steric asymmetry

For NO–Ar, S exhibits a striking undulatory character at a collision energy of $E_{tr} = 475\ \mathrm{cm}^{-1}$, as shown in Fig. 1. When the orientation field is applied such that the N-end of the NO molecule is favored to point towards the Ar, the collision yields mostly $\Delta j =$ even. For O-end collisions, $\Delta j =$ odd is preferred [1,4,5,16]. This effect is seen for both spin–orbit conserving and spin–orbit changing collisions. The value of the steric asymmetry as a function of $\Delta j = j' - j$ for collisions of both OH and NO with Ar turns out to be insensitive of ϵ'. In the search for a better understanding of the striking oscillatory behavior of S, a semi-quantum mechanical hard shell model is being developed. Application of this model [17] to NO–Ar yields a similar undulatory behavior, but S carries an improper sign compared to measurements and quantum mechanically calculated values. Application of this model to OH–Ar yields the "proper" sign of S compared to the reported measured and calculated values [6,13].

To render insight into the "proper" sign of S, we turn to a recent study of van Beek et al. [6]. This study reports about the steric dependence of (state resolved) rotational energy transfer for the 'hetero' nuclear OH–Ar collision system. A hexapole is used to select the OH beam predominantly in a $j = \overline{\Omega} = \overline{m}_j = \frac{3}{2}$, $\epsilon_u(f)$ state, that is oriented in the collision region using an electric field $\mathbf{E}$. In accordance with their experimental convention Schreel et al. and later van Beek et al. define S such that according to Eq. (1) the O-end of the molecule corresponds to the head, while the H-end refers to the tail [6,13]. At a collision energy of $746\ \mathrm{cm}^{-1}$, van Beek et al. observed a general trend that was independent of the final spin–orbit state and of the Λ-doublet component. For excitation to low rotational states, S is typically small and positive, indicating a weak O-end preference. For excitation to a higher rotational state, S becomes large and negative, implying that H-end collisions are preferred. A simple ball and stick model explains this behavior. In the case of "tail" (H-end) orientation of the molecule, the H atom will have a much higher probability of pointing towards the

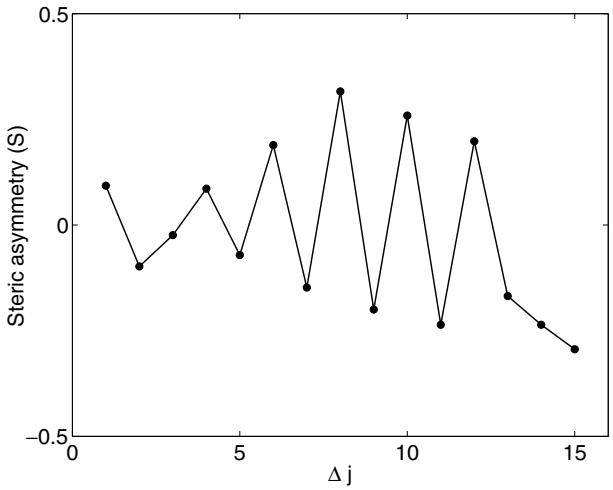

Fig. 1. Experimental steric asymmetry ($\epsilon = \epsilon_u = \epsilon' = -1$) as a function of $\Delta j = j' - j$ for spin–orbit conserving collisions of NO with Ar at a collision energy of $E_{tr} = 475\ cm^{-1}$ [16]. Earlier data [5] have been improved using a flux to density transformation that transformed LIF intensities into proper state-to-state cross-sections. This treatment overall enhanced the amplitude of S, but not its sign.

Ar atom. For the "head" orientation, the O-end of the molecule is likely to shield off the H-end from the Ar atom. Due to the shape of the OH molecule, the torque that is exerted on the H-end ("stick") is much larger than that on the O-end ("ball") at a similar relative velocity ($\mathbf{v}_{rel}$). A large torque results in a high rotational excitation, as was noticed for the dependence of S on j' by van Beek et al. [6].

In addition to van Beek's measurements, close coupling scattering calculations for OH–Ar were carried out on the CEPA [18] and on the UMP4 (unrestricted fourth-order Møller–Plesset [8]) ab initio OH–Ar potential energy surfaces (PESs). For both PESs, the steric asymmetry as well as the integral inelastic cross-sections (depending on $\overline{\Omega}'$ and ϵ') have been calculated with HIBRIDON [7]. These results agree reasonably with the experimental values. A close inspection of the HIBRIDON code, however, shows that the orientations that correspond with HIBRIDON's "heads" and "tails" labels relate directly to the choice of the Jacobi coordinates **R** (displacement vector between atom A and molecule BC), $\hat{\mathbf{r}}$ (BC bond vector, that points from the tail C towards the head B) and ϑ (angle between $\hat{\mathbf{r}}$ and **R**). For NO–Ar, $\vartheta = 0$ corresponds with collinear Ar–NO configuration for both the CEPA [19] and the CCSD(T) [20] PESs. These PESs have been used to calculate scattering cross-sections and steric asymmetries with HIBRIDON [7] and with a (modified [1]) version of MOLSCAT [21]. In the case of OH, for both the CEPA and the UMP4 PESs, $\vartheta = 0$ corresponds to the linear Ar–HO geometry. This means that HIBRIDON assumes the H-end of the OH molecule as being the head, while the H-end of the molecule is defined by van Beek and coworkers as being the tail of the molecule. Without adapting HIBRIDON's definition to the experimental one, HIBRIDON is expected to provide results for S that carry a sign opposite to that of van Beek's experimental value, which was reported not to be the case [6].

To investigate whether the theoretical results reported by van Beek et al. carry the "proper" sign, steric asymmetries have been recalculated for OH ($v = 0$, $X^2\Pi_{3/2}$ $j = \frac{3}{2}$) scattered by Ar at a collision energy of 451 and 746 cm^{-1} on the UMP4 PESs. Calculations have been performed on three different cases: 94% $\overline{m}_j = \frac{3}{2}$ and 6% $\overline{m}_j = \frac{1}{2}$, 100% $\overline{m}_j = \frac{3}{2}$ and on a "hard shell" assuming 100% $\overline{m}_j = \frac{3}{2}$. The calculated steric asymmetries for three cases are shown in Table 1. From this table, one immediately notices a reasonable agreement between the experimental and all theoretical amplitudes of S, resulting from the UMP4 PESs. The present calculations yield an overall smaller amplitude for S at high j', than the measured values. As far as the sign of S is concerned, there is a striking opposite trend for the experimental values (S^E) compared to our theoretically calculated values (S^C) based on the UMP4 PESs. The steric asymmetry as defined in the experiment $S^E = (\sigma^{OH} - \sigma^{HO})/(\sigma^{OH} + \sigma^{HO})$ should carry a sign opposite to that calculated by HIBRIDON reflecting the parameterization of the UMP4 and CEPA PESs $S^C = (\sigma^{HO} - \sigma^{OH})/(\sigma^{HO} + \sigma^{OH}) = -S^E$. To advance quantum mechanical calculations closer to the ball and stick model, a hard shell alike system was mimicked for the OH–Ar system. To damp the attractive well, the sum potential (V_{sum}) was multiplied with

$$\tfrac{1}{2}[1 - \tanh\{3(R - 7.08)\}] \tag{10}$$

and also set $V_{dif} = 0$. It should be noted that in this case R is in Bohr. The amplitude of S^C for the "hard shell" alike calculations (shown in Table 1) is much stronger than that for the full PESs, as it is no longer diluted by the attractive part of $V_{sum}(R)$. S^E shows a proper negative sign for nearly all rotational excited states, in accordance with the ball and

Table 1
Experimental and theoretical steric asymmetries for rotational excitation of OH $X^2\Pi_{3/2}, j = \frac{3}{2}, \epsilon = -1$ in collisions with Ar at a collision energy of 746 cm^{-1}

Final state[a]			Steric asymmetry (%)				
			Experimental	Theoretical results on UMP4			"Hard shell"
$\overline{\Omega}'$	J'	ϵ'	van Beek[b]	94% $\overline{m}_j = \frac{3}{2}$[b]	94% $\overline{m}_j = \frac{3}{2}$[c]	100% $\overline{m}_j = \frac{3}{2}$[c]	100% $\overline{m}_j = \frac{3}{2}$[c]
$\frac{3}{2}$	$\frac{5}{2}$	e	1.4 ± 0.4	5.8	4.9	5.0	−21.4
		f	5.0 ± 1.9	4.9	10.7	11.2	−22.5
	$\frac{7}{2}$	e	-19.3 ± 1.0	−5.7	−12.1	−14.0	−22.2
		f	-1.3 ± 3.5	−1.2	0	0.5	−20.5
	$\frac{9}{2}$	e	-78.1 ± 1.3	−82.1	−12.1	−52.6	−50.6
		f	-23.2 ± 25.4	−47.5	−5.8	−10.6	−36.8
$\frac{1}{2}$	$\frac{1}{2}$	e	9.6 ± 1.8	11.8	0.4	0.5	9.1
		f	22.3 ± 3.1	−1.3	−7.5	−10.8	8.4
	$\frac{3}{2}$	e	2.9 ± 2.2[d]	3.7	−3.6	−11.6	−25.4
		f	-24.1 ± 2.6	−18.1	−1.3	−3.3	−35.3
	$\frac{5}{2}$	e	2.9 ± 2.2[d]	−40.7	−1.3	−8.9	−34.6
		f	-25.8 ± 3.0	−34.6	−7.5	−10.9	−28.3

It should be noted that the published [6] steric asymmetry is defined as $S^{\mathrm{E}} = (\sigma^{\mathrm{OH}} - \sigma^{\mathrm{HO}})/(\sigma^{\mathrm{OH}} + \sigma^{\mathrm{HO}})$, while the present calculations use the definition that follows from HIBRIDON in combination with the UMP4 and CEPA parameterization [8,18]: $S^{\mathrm{C}} = (\sigma^{\mathrm{HO}} - \sigma^{\mathrm{OH}})/(\sigma^{\mathrm{HO}} + \sigma^{\mathrm{OH}}) = -S^{\mathrm{E}}$.

[a] The label "e" corresponds with $\epsilon' = 1$ and "f" corresponds with $\epsilon' = -1$.

[b] Values from [6].

[c] Present calculations, this work.

[d] Transitions for scattering into the $\frac{1}{2}, \frac{3}{2}$, e and $\frac{1}{2}, \frac{5}{2}$, e level cannot be separately resolved. Accordingly, the steric asymmetries in the experimental column is the combined steric asymmetry for the $\frac{3}{2}, \frac{3}{2}$, f $\rightarrow \frac{1}{2}, \frac{3}{2}$, e and $\frac{3}{2}, \frac{3}{2}$, f $\rightarrow \frac{1}{2}, \frac{5}{2}$, e excitations.

stick model. Only the spin–orbit changing transition $j = \frac{3}{2}, \overline{\Omega} = \frac{3}{2}, E \rightarrow j' = \frac{1}{2}, \overline{\Omega} = \frac{3}{2}, \epsilon' = -1$ carries an opposite sign for S^{E}. Comparison of the results of the "hard shell" calculation with the outcome of the ball and stick model makes it plausible that the present HIBRIDON calculations provide the improper sign for S^{C}. One would not expect that the O-end is preferred to yield high rotational states. Steric asymmetries are shown in Table 1 and Fig. 2.

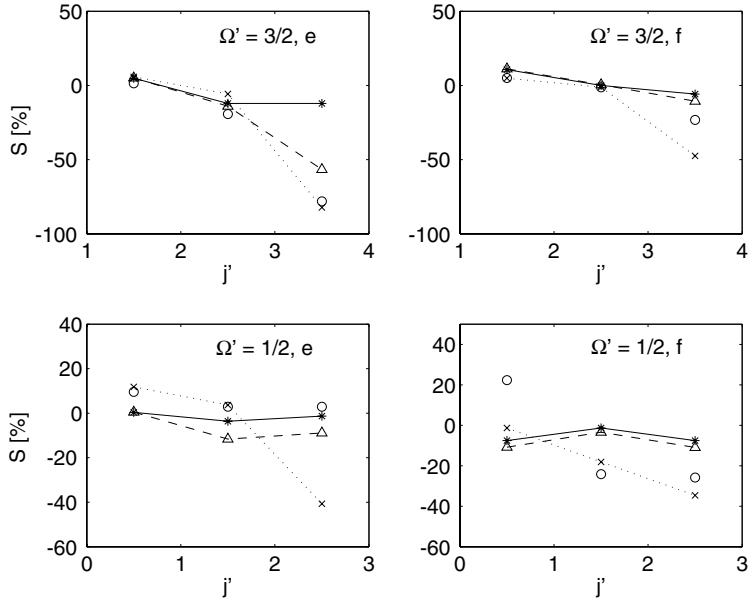

Fig. 2. Steric asymmetries as a function of the final state of OH–Ar at $E_{\mathrm{tr}} = 781$ cm^{-1}. Note that the experimental steric asymmetry is taken conform [13] and is defined as $S^{\mathrm{E}} = (\sigma^{\mathrm{OH}} - \sigma^{\mathrm{HO}})/(\sigma^{\mathrm{OH}} + \sigma^{\mathrm{HO}})$, while the present theoretical results are plotted according to the definition following HIBRIDON parameterization and UMP4 and CEPA PESs $S^{\mathrm{C}} = (\sigma^{\mathrm{HO}} - \sigma^{\mathrm{OH}})/(\sigma^{\mathrm{HO}} + \sigma^{\mathrm{OH}}) = -S^{\mathrm{E}}$. Experimental values [6] are indicated with open circles "○", theoretical results on the UMP4 PESs with 94% $\overline{m}_j = \frac{3}{2}$ are given with a dotted line and a cross "×" [6]. Theoretical results from our work [94% $\overline{m}_j = \frac{3}{2}$ and 6% $\overline{m}_j = \frac{1}{2}$] and [100% $\overline{m}_j = \frac{3}{2}$] are respectively given by a solid line and a star "*" and a dashed line in combination with a triangle "△".

Table 2
Theoretical integral state-to-state cross-sections (Å^2) for rotational excitation of OH $X\,^2\Pi_{3/2}, j = \frac{3}{2}$, f in collisions with Ar are listed for comparison

Final state			$E_{col} = 451$ cm^{-1}		$E_{col} = 746$ cm^{-1}	
Ω'	J'	ϵ'	Pure[a]	Pure[b]	Pure[a]	pure[b]
$\frac{3}{2}$	$\frac{3}{2}$	e	16.5	16.50	11.5	11.40
		f	–	–	–	–
	$\frac{5}{2}$	e	11.8	11.80	11.2	11.20
		f	2.42	2.42	1.62	1.62
	$\frac{7}{2}$	e	2.19	2.19	2.15	2.13
		f	0.350	0.35	0.756	0.75
	$\frac{9}{2}$	e	0.553	0.53	0.703	0.70
		f	0.013	0.01	0.090	0.09
$\frac{1}{2}$	$\frac{1}{2}$	e	2.10	2.10	2.19	2.22
		f	0.238	0.24	0.197	0.20
	$\frac{3}{2}$	e	0.524	0.52	0.826	0.83
		f	0.711	0.71	0.927	0.90
	$\frac{5}{2}$	e	0.458	0.46	0.598	0.60
		f	0.458	0.46	0.598	0.60
		Total	37.86	37.73	32.76	32.64

A collision energy of 451 and 746 cm^{-1} has been used. All calculations are based on the UMP4 PESs.
[a] Present result.
[b] van Beek et al. [22].

As there is not a perfect agreement among the absolute theoretical results for S^C on the UMP4 PESs as obtained in this study and in [6], integral state-to-state cross-sections have been calculated to test the integration procedure. Truncating the summation over the coupled T-matrix elements in Eq. (7) at $J > 101$ ($E_{col} = 451$ cm^{-1}) and at $J > 130$ ($E_{col} = 781$ cm^{-1}), perfect agreement (Table 2) with "pure" theoretical integral state-to-state cross-sections is reported [22]. We have no answer on the question why our results for S^C differ this much from previous calculations [6].

Although the NO–Ar system is more homo-nuclear than OH–Ar, one can also apply the ball and stick model on this system. The O-end is more round than the N-end, that extends further from the center-of-mass. From a ball and stick model, one would conclude that the N-end will be preferred for high rotational states, but this is not what was found in earlier experiments and theory [1,4,5]. The only exception in respect to this finding is the first (erroneous) measurement of S by van Leuken, that did not correspond with theoretical results in the same paper [1]. Except this experimental result, all published results for S of NO–Ar collisions show a negative value for S for high rotational states. This indicates that molecules with high rotational states mostly carry back on O-end collisions. There is no satisfactory explanation for this effect that goes against ones natural wit.

4. Theory

4.1. The coupled Schrödinger equation, T-matrix and scattering amplitude

The CMS in which the collision of an atom A and a diatomic molecule BC can be described allows for two distinguished conventions regarding the definition of $\boldsymbol{R}$. The convention followed in most theoretical procedures [7,12,21] uses the displacement vector of the center of A in respect to the CM of BC:

$$\mathbf{R} = \mathbf{R}_{A-BC} = \mathbf{R}_A - \mathbf{R}_{BC}. \tag{11}$$

Alternatively, the "opposite" convention

$$\mathbf{R} = \mathbf{R}_{BC-A} = \mathbf{R}_{BC} - \mathbf{R}_A \tag{12}$$

provides an equally well-suited definition of $\mathbf{R}$. Both conventions are illustrated in Fig. 3. For the simplest (elastic) case of the collision between the two particles A and BC, the scattering matrix $\boldsymbol{T}$ reduces to a row of dimensionless scalars. The value of these scalars does not bear any relation upon the chosen convention of $\boldsymbol{R}$ (see, e.g. [10,23,24]). In the case of rotationally inelastic scattering this also holds for the value of the CMS scattering angles (θ, ϕ), whereas the scattering matrix and the scattering amplitude could depend on the choice of $\mathbf{R} = \mathbf{R}_{A-BC}$ or $\mathbf{R} = \mathbf{R}_{BC-A}$. In this section,

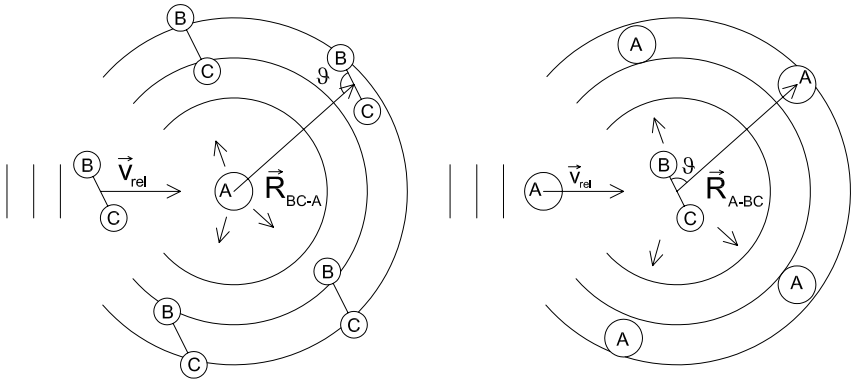

Fig. 3. Incoming planar wave and outgoing spherical wave that represents a state-to-state collision between a molecule BC and an atom A. The right panel depicts this process in the (A–BC) CMS with $\mathbf{R} = \mathbf{R}_{A-BC}$, the left panel reflects the so-called inverted CMS with $\mathbf{R} = \mathbf{R}_{BC-A} = -\mathbf{R}_{A-BC}$. This figure elucidates that a change from one convention to another also alters the Jacobi angles ϑ. The Jacobi angles for both cases are related as $\vartheta_{A-BC} = \pi - \vartheta_{BC-A}$. Note that the ϑ has to be distinguished from the CMS scattering angle θ which denotes the angle between the outgoing and incoming wave vectors $\hat{k}$ and $\hat{k}'$.

we will show that a change of convention will not cause any problem in relation to the state-to-state differential and integral cross-sections, as long as one refrains from orientational dependence.

To elucidate the influence of the choice of $\mathbf{R}_{A-BC}$ or $\mathbf{R}_{BC-A}$ on the T-matrix, the set of (close) coupled differential equations that substantiate the Schrödinger equation of the scattering problem will be considered. When denoting the total wavefunction as

$$\mathbf{\Psi}^{J,M_J}_{j,l,\overline{\Omega},\epsilon}(\hat{\mathbf{r}},\mathbf{R}) = \sum_{j',l',\overline{\Omega}',\epsilon'} \frac{1}{R} U^{J,M_J}_{j',l',\overline{\Omega}',\epsilon'}(R) \sum_{m'_j,m'_l} \langle j', m'_j, l', m'_l | J, M_J\rangle |j', m'_j, \overline{\Omega}', \epsilon'\rangle Y_{l',m'_l}(\hat{\mathbf{R}}), \tag{13}$$

the set of close coupled equations that has to be solved numerically becomes [11,12]

$$\left[-\frac{\hbar^2}{2\mu}\frac{\mathrm{d}^2}{\mathrm{d}R^2} + \frac{\hbar^2 l(l+1)}{2\mu R^2} + \langle j, l, \overline{\Omega}, \epsilon, J, M_J | V | j, l, \overline{\Omega}, \epsilon, J, M_J\rangle \right] U^{J,M_J}_{j,l,\overline{\Omega},\epsilon}(R) + \sum_{j',l',\overline{\Omega}',\epsilon'} (1 - \delta_{j,j'}\delta_{l,l'}\delta_{\overline{\Omega},\overline{\Omega}'}\delta_{\epsilon,\epsilon'})$$
$$\times \langle j', l', \overline{\Omega}', \epsilon', J, M_J | V | j, l, \overline{\Omega}, \epsilon, J, M_J\rangle U^{J,M_J}_{j',l',\overline{\Omega}',\epsilon'}(R) = 0. \tag{14}$$

The radial part of the wavefunction of Eq. (13) obeys to the boundary condition

$$\lim_{R\to\infty} U^{J,M_J}_{j',l',\overline{\Omega}',\epsilon'}(R) = \delta_{j,j'}\delta_{l,l'}\delta_{\overline{\Omega},\overline{\Omega}'}\delta_{\epsilon,\epsilon'} \exp\left[-\mathrm{i}\left(k_{j,\overline{\Omega}}\cdot R - l\frac{\pi}{2}\right)\right] \sqrt{\frac{k_{j',\overline{\Omega}'}}{k_{j,\overline{\Omega}}}} \left(\delta_{j,j'}\delta_{l,l'}\delta_{\overline{\Omega},\overline{\Omega}'}\delta_{\epsilon,\epsilon'} - T^J_{j',l',\overline{\Omega}',\epsilon';j,l,\overline{\Omega},\epsilon}\right)$$
$$\times \exp\left[\mathrm{i}\left(k_{j',\overline{\Omega}}\cdot R - l'\frac{\pi}{2}\right)\right] = 0. \tag{15}$$

When one assumes that the equations above correspond to the convention $\mathbf{R} \equiv \mathbf{R}_{A-BC}$, Eq. (14) can easily be adapted to the case $\mathbf{R} = \mathbf{R}_{BC-A}$, applying the inversion operator $i_{\mathbf{R}}$

$$Y_{l,m_l}(\hat{\mathbf{R}}_{A-BC}) = i_{\mathbf{R}} Y_{l,m_l}(\hat{\mathbf{R}}_{BC-A}) = (-1)^l Y_{l,m_l}(\hat{\mathbf{R}}_{BC-A}). \tag{16}$$

Eq. (16) leads to

$$\left[-\frac{\hbar^2}{2\mu}\frac{\mathrm{d}^2}{\mathrm{d}R^2} + \frac{\hbar^2 l(l+1)}{2\mu R^2} + \langle j, l, \overline{\Omega}, \epsilon, J, M_J | V | j, l, \overline{\Omega}, \epsilon, J, M_J\rangle \right] U^{J,M_J}_{j,l,\overline{\Omega},\epsilon}(R_{BC-A}) + \sum_{j',l',\overline{\Omega}',\epsilon'} (1 - \delta_{j,j'}\delta_{l,l'}\delta_{\overline{\Omega},\overline{\Omega}'}\delta_{\epsilon,\epsilon'})$$
$$\times \langle j', l', \overline{\Omega}', \epsilon', J, M_J | V | j, l, \overline{\Omega}, \epsilon, J, M_J\rangle (-1)^{l+l'} U^{J,M_J}_{j',l',\overline{\Omega}',\epsilon'}(R_{BC-A}) = 0. \tag{17}$$

Application of the boundary condition of Eq. (15) onto the solutions of the coupled equations Eqs. (14) and (17) leads immediately to

$$T^{(J),A-BC}_{j',l',\overline{\Omega}',\epsilon';j,l,\overline{\Omega},\epsilon} \equiv T^J_{j',l',\overline{\Omega}',\epsilon';j,l,\overline{\Omega},\epsilon} = (-1)^{l+l'} T^{(J),BC-A}_{j',l',\overline{\Omega}',\epsilon';j,l,\overline{\Omega},\epsilon}. \tag{18}$$

As elucidated in Eq. (5) T-matrix elements $T^{(J),\mathrm{A-BC}}_{j',l',\overline{\Omega}',\epsilon';j,l,\overline{\Omega},\epsilon}$ and $T^{(J),\mathrm{BC-A}}_{j',l',\overline{\Omega}',\epsilon';j,l,\overline{\Omega},\epsilon}$ may be uncoupled, for example, to the regular collision frame or to the reversed collision frame. Substitution of Eq. (18) into Eq. (7) yields the scattering amplitude in the (BC–A) collision frame (Fig. 4):

$$f^{\mathrm{BC-A}}_{j,m_j,\overline{\Omega},\epsilon\to j',m'_j,\overline{\Omega}',\epsilon'}(\hat{\mathbf{k}}') = \sqrt{\pi}\sum_{J,l,l'}(2l+1)^{1/2}(2J+1)i^{l-l'}\begin{pmatrix} j & J & l \\ m_j & -m_j & 0\end{pmatrix}\begin{pmatrix} j' & J & l' \\ m'_j & -m_j & m_j-m'_j\end{pmatrix} \times Y_{l',m_j-m'_j}(\hat{\mathbf{k}}')(-1)^{l+l'}T^{(J),\mathrm{A-BC}}_{j',l',\overline{\Omega}',\epsilon';j,l,\overline{\Omega},\epsilon}. \tag{19}$$

As noted by Alexander [3], the absence of coupling between incoming and outgoing states of different total parity leads to

$$T^{(J)}_{j',l',\overline{\Omega}',\epsilon';j,l,\overline{\Omega},\epsilon} = 0 \quad \text{unless } (-1)^{l+l'} = \epsilon\epsilon'(-1)^{j'-j}. \tag{20}$$

Application of Eq. (20) in Eq. (19) yields

$$f^{\mathrm{BC-A}}_{j,m_j,\overline{\Omega},\epsilon\to j',m'_j,\overline{\Omega}',\epsilon'}(\hat{\mathbf{k}}') = f^{\mathrm{A-BC}}_{j,m_j,\overline{\Omega},\epsilon\to j',m'_j,\overline{\Omega}',\epsilon'}(\hat{\mathbf{k}}')\epsilon\epsilon'(-1)^{j'-j}. \tag{21}$$

As illustrated in Fig. 4, the relation between the scattering amplitudes of Eq. (21) remains valid either within the regular or within the reversed collision frame.

4.2. The m_j-dependent state-to-state collision cross-section for non-oriented molecules

Application of Eq. (21) into Eq. (8) with $\beta(E) = 0$ and substituting this result in Eq. (9) gives

$$\mathrm{d}\sigma_{j,m_j,\overline{\Omega},\epsilon\to j',m'_j,\overline{\Omega}',\epsilon'}/\mathrm{d}\omega = \frac{1}{k^2}\left|f^{\mathrm{A-BC}}_{j,m_j,\overline{\Omega},\epsilon\to j',m'_j,\overline{\Omega}',\epsilon'}(\hat{\mathbf{k}}')\right|^2 = \frac{1}{k^2}\left|f^{\mathrm{BC-A}}_{j,m_j,\overline{\Omega},\epsilon\to j',m'_j,\overline{\Omega}',\epsilon'}(\hat{\mathbf{k}}')\right|^2. \tag{22}$$

Depending on the A–BC or BC–A sign convention for the intermolecular displacement vector, the scattering amplitudes and coupled T-matrix elements do not have to be equal in sign. Eq. (22) however, shows that their relation to the differential cross-section $\mathrm{d}\sigma_{j,m_j,\overline{\Omega},\epsilon\to j',m'_j,\overline{\Omega}',\epsilon'}/\mathrm{d}\omega$ does not depend on the choice of the A–BC or BC–A convention. In addition to this, the insensitivity of the differential cross-section to the sense of rotation in the (regular or reversed) collision frame $\mathrm{d}\sigma_{j,m_j,\overline{\Omega},\epsilon\to j',m'_j,\overline{\Omega}',\epsilon'}/\mathrm{d}\omega = \mathrm{d}\sigma_{j,-m_j,\overline{\Omega},\epsilon\to j',-m'_j,\overline{\Omega}',\epsilon'}/\mathrm{d}\omega$ [3] infers that non-oriented molecules do not yield a different outcome for scattering calculations in the collision and in the reversed collision frame.

Not only the dependence of the differential cross-section on the scattering angle that is treated above, but also the dependence of the total cross-section on the final state has experimentally been investigated [16,22]. The total cross-section can be obtained by numerical integration of the differential cross-section $\mathrm{d}\sigma_{j,m_j,\overline{\Omega},\epsilon\to j',m'_j,\overline{\Omega}',\epsilon'}/\mathrm{d}\omega$ over the full range of $\mathrm{d}\omega$. The rapid diffraction oscillations in the differential cross-section can cause this integration to be cumbersome [3]. Alternatively, the integral cross-section can be obtained directly as an exact summation over products of

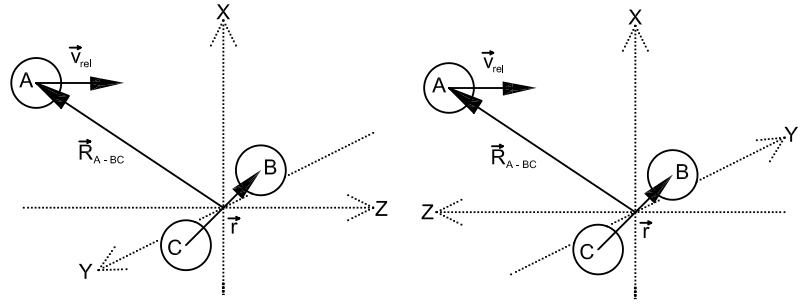

Fig. 4. Two convenient CM inertial frames in which a collision between a molecule and an atom can be described. In the regular collision frame (left panel) the relative velocity $\mathbf{v}_{\mathrm{rel}}$ is directed parallel to the Z axis of m_j and m_l quantization. In the reversed collision frame (right panel) $\mathbf{v}_{\mathrm{rel}}$ is directed anti-parallel to the Z-axis, thus giving the opposite sign for all m_j and m_l quantum numbers. Both panels depict the A–BC CM system with $\mathbf{R} = \mathbf{R}_{\mathrm{A-BC}}$. The T-matrix elements themselves do not depend on the choice of the coordinate frame. Eq. (29) of [25] relates the scattering amplitudes to the T-matrix for arbitrary orientation of the coordinate frame of which the Z axis provides the quantization axis. Application of this expression leads to an extra multiplication factor $(-1)^{l+l'}$ to the T matrix elements in Eq. (7) when one applies this formula for the reversed collision frame. Note that the same multiplication factor $(-1)^{l+l'}$ appears in Eq. (18) when one switches from the (A–BC) CMS ($\mathbf{R} = \mathbf{R}_{\mathrm{A-BC}}$) to the inverted CMS ($\mathbf{R} = \mathbf{R}_{\mathrm{BC-A}}$).

T-matrix elements by making use of the orthogonality properties of the spherical harmonics $Y_{l',m_j-m'_j}(\hat{\mathbf{k}}')$. The contributions to this summation are restricted by Eq. (20):

$$\sigma_{j,m_j,\overline{\Omega},\epsilon\to j',m'_j,\overline{\Omega}',\epsilon'} = \frac{\pi}{k^2}\sum_{J,J'l,l',l'',(l+l'' \text{ even})} \sqrt{2l+1}\sqrt{2l''+1}(2J+1)(2J'+1)\begin{pmatrix} j & J & l \\ m_j & -m_j & 0\end{pmatrix}\begin{pmatrix} j' & J' & l'' \\ m_j & -m_j & 0\end{pmatrix} \times \begin{pmatrix} j' & J & l' \\ m'_j & -m_j & m_j-m'_j\end{pmatrix}\begin{pmatrix} j' & J' & l' \\ m'_j & -m_j & m_j-m'_j\end{pmatrix}(-1)^{(l-l'')/2}\ T^{J*}_{j',l',\overline{\Omega}',\epsilon';j,l'',\overline{\Omega},\epsilon} T^{J'}_{j',l',\overline{\Omega}',\epsilon';j,l,\overline{\Omega},\epsilon}. \tag{23}$$

Since the detection selectivity for the scattered BC molecules is typically too low to resolve m'_j, the experimental observation relates to

$$\sigma_{j,m_j,\overline{\Omega},\epsilon\to j',\overline{\Omega}',\epsilon'} = \sum_{m'_j}\sigma_{j,m_j,\overline{\Omega},\epsilon\to j',m'_j,\overline{\Omega}',\epsilon'}. \tag{24}$$

This allows one to contract Eq. (23) to

$$\sigma_{j,m_j,\overline{\Omega},\epsilon\to j',\overline{\Omega}',\epsilon'} = \frac{\pi}{k^2}\sum_{J,l,l',l'',(l+l'' \text{ even})} C^J_{l,l''}(j,m_j)(-1)^{(l-l'')/2}\ T^{J*}_{j',l',\overline{\Omega}',\epsilon';j,l'',\overline{\Omega},\epsilon} T^{J}_{j',l',\overline{\Omega}',\epsilon';j,l,\overline{\Omega},\epsilon}, \tag{25}$$

with

$$C^J_{l,l''}(j,m_j) \equiv \sqrt{2l+1}\sqrt{2l''+1}(2J+1)\begin{pmatrix} j & J & l \\ m_j & -m_j & 0\end{pmatrix}\begin{pmatrix} j & J & l'' \\ m_j & -m_j & 0\end{pmatrix}. \tag{26}$$

Note that $C^J_{l,l''}(j,m_j) = C^J_{l'',l}(j,m_j) = (-1)^{l+l'}C^J_{l,l''}(j,-m_j)$. In experiments with NO [1,5] the initial state is selected in $j=\frac{1}{2}$, which leads to $\overline{m}_j=\frac{1}{2}$. Because of Eq. (26), $l''=l'=J\pm\frac{1}{2}$:

$$C^J_{J-\frac{1}{2},J-\frac{1}{2}}\left(\frac{1}{2},m_j\right) = C^J_{J+\frac{1}{2},J+\frac{1}{2}}\left(\frac{1}{2},m_j\right) = \frac{2J+1}{2}. \tag{27}$$

Combination of Eq. (27) with Eq. (23) gives a convenient expression for the integral cross-section:

$$\sigma_{\frac{1}{2},m_j,\overline{\Omega},\epsilon\to j',\overline{\Omega}',\epsilon'} = \frac{\pi}{2k^2}\sum_{J,l',l=J\pm\frac{1}{2}}(2J+1)\left[T^{J*}_{j',l',\overline{\Omega}',\epsilon';\frac{1}{2},l,\overline{\Omega},\epsilon}T^{J}_{j',l',\overline{\Omega}',\epsilon';\frac{1}{2},l,\overline{\Omega},\epsilon}\right]. \tag{28}$$

The explicit expression for the integral cross-section of Eq. (28) for $j=\frac{3}{2}$ with $\overline{m}_j=\frac{3}{2}$ and/or $\overline{m}_j=\frac{1}{2}$ (OH experiments [13,14,22]) contains a more extended summation over l and l''. Non-zero contributions may occur in Eq. (26) when $l=l''=J\pm\frac{3}{2}$, $l=l''=J\pm\frac{1}{2}$ and $l=J\pm\frac{3}{2}$, $l''=J\mp\frac{1}{2}$ or $l=J\mp\frac{1}{2}$, $l''=J\pm\frac{3}{2}$. Application of Eq. (26) for $\overline{m}_j=\frac{3}{2}$ leads to

$$C^J_{J\pm\frac{3}{2},J\pm\frac{3}{2}}\left(\frac{3}{2},\frac{3}{2}\right) = \frac{(2J+1\mp2)(2J+1)}{8(2J+1\pm1)}, \tag{29}$$

$$C^J_{J\pm\frac{1}{2},J\pm\frac{1}{2}}\left(\frac{3}{2},\frac{3}{2}\right) = \frac{3(2J+1\mp2)(2J+1)}{8(2J+1\mp1)}, \tag{30}$$

$$C^J_{J\pm\frac{3}{2},J\mp\frac{1}{2}}\left(\frac{3}{2},\frac{3}{2}\right) = C^J_{J\mp\frac{1}{2},J\pm\frac{3}{2}}\left(\frac{3}{2},\frac{3}{2}\right) = \frac{\sqrt{3(2J-1)(2J+3)}(2J+1)}{8(2J+1\pm1)}. \tag{31}$$

The integral cross-section can be calculated after substitution of Eqs. (29)–(31) in Eq. (25):

$$\sigma_{\frac{3}{2},\overline{m}_j=\frac{3}{2},\overline{\Omega},\epsilon\to j',\overline{\Omega}',\epsilon'} = \frac{\pi}{2k^2}\sum_{l',J}(2J+1)\left[\frac{1}{4}\sum_{l=J\pm\frac{3}{2}}\frac{(2J+1\mp1)}{(2J+1\pm1)}T^{J*}_{j',l',\overline{\Omega}',\epsilon';\frac{3}{2},l,\overline{\Omega},\epsilon}T^{J}_{j',l',\overline{\Omega}',\epsilon';\frac{3}{2},l,\overline{\Omega},\epsilon} + \frac{3}{4}\sum_{l=J\pm\frac{1}{2}}\frac{(2J+1\mp2)}{(2J+1\mp1)}T^{J*}_{j',l',\overline{\Omega}',\epsilon';\frac{3}{2},l,\overline{\Omega},\epsilon}T^{J}_{j',l',\overline{\Omega}',\epsilon';\frac{3}{2},l,\overline{\Omega},\epsilon} - \frac{\sqrt{3}}{2}\sum_{l=J\pm\frac{3}{2},l''=J\mp\frac{1}{2}}\frac{\sqrt{(2J-1)(2J+3)}}{2J+1\pm1} \times \mathrm{Re}\left(T^{J*}_{j',l',\overline{\Omega}',\epsilon';\frac{3}{2},l,\overline{\Omega},\epsilon}T^{J}_{j',l',\overline{\Omega}',\epsilon';\frac{3}{2},l'',\overline{\Omega},\epsilon}\right)\right]. \tag{32}$$

To complete the treatment for OH, application of Eq. (26) for $\overline{m}_j = \frac{1}{2}$ leads to

$$C^J_{J\pm\frac{3}{2},J\pm\frac{3}{2}}\left(\frac{3}{2},\frac{1}{2}\right) = \frac{3(2J+1\pm 2)(2J+1)}{8(2J+1\pm 1)}, \tag{33}$$

$$C^J_{J\pm\frac{1}{2},J\pm\frac{1}{2}}\left(\frac{3}{2},\frac{1}{2}\right) = \frac{(2J+1\pm 2)(2J+1)}{8(2J+1\mp 1)}, \tag{34}$$

$$C^J_{J\pm\frac{3}{2},J\mp\frac{1}{2}}\left(\frac{3}{2},\frac{1}{2}\right) = C^J_{J\mp\frac{1}{2},J\pm\frac{3}{2}}\left(\frac{3}{2},\frac{1}{2}\right) = \frac{-\sqrt{3(2J-1)(2J+3)}(2J+1)}{8(2J+1\pm 1)}. \tag{35}$$

The total cross-section can be calculated after substitution of Eqs. (33)–(35) in Eq. (25):

$$\begin{aligned}\sigma_{\frac{3}{2},\overline{m}_j=\frac{1}{2},\overline{\Omega},\epsilon\to j',\overline{\Omega}',\epsilon'} = \frac{\pi}{2k^2}\sum_{l',J}(2J+1)\Bigg[&\frac{3}{4}\sum_{l=J\pm\frac{3}{2}}\frac{(2J+1\pm 2)}{(2J+1\pm 1)}T^{J*}_{j',l',\overline{\Omega}',\epsilon';\frac{3}{2},l,\overline{\Omega},\epsilon}T^{J}_{j',l',\overline{\Omega}',\epsilon';\frac{3}{2},l,\overline{\Omega},\epsilon}\\ &+\frac{1}{4}\sum_{l=J\pm\frac{1}{2}}\frac{(2J+1\pm 2)}{(2J+1\mp 1)}T^{J*}_{j',l',\overline{\Omega}',\epsilon';\frac{3}{2},l,\overline{\Omega},\epsilon}T^{J}_{j',l',\overline{\Omega}',\epsilon';\frac{3}{2},l,\overline{\Omega},\epsilon}\\ &+\frac{\sqrt{3}}{2}\sum_{l=J\pm\frac{3}{2},l''=J\mp\frac{1}{2}}\frac{\sqrt{(2J-1)(2J+3)}}{2J+1\pm 1}\mathrm{Re}\left(T^{J*}_{j',l',\overline{\Omega}',\epsilon';\frac{3}{2},l,\overline{\Omega},\epsilon}T^{J}_{j',l',\overline{\Omega}',\epsilon';\frac{3}{2},l'',\overline{\Omega},\epsilon}\right)\Bigg].\end{aligned} \tag{36}$$

4.3. The m_j-dependent state-to-state collision cross-section for oriented molecules

The next issue that will be addressed is whether the choice for either the $\mathbf{R}_{\mathrm{A-BC}}$ or the $\mathbf{R}_{\mathrm{BC-A}}$ displacement vector affects the orientational dependence of the collision cross-section. As a first step notice that $|j,\pm m_j,\pm\overline{\Omega}\rangle$ and $|j,\mp m_j,\mp\overline{\Omega}\rangle$ correspond to wavefunctions that, respectively, favor head and tail orientation of the BC molecule along the Z-axis (which is the quantization axis). As pointed out by Loesch [26] collisions on the C-end of the BC molecule are preferred when the B-end favors to point along $\mathbf{v}_{\mathrm{rel}}$ in the (A–BC) CMS. In the (BC–A) CMS used by Stolte et al. [27,28], collisions impinging onto the B-end of the BC molecule are preferred when the B-end favors points along $\mathbf{v}_{\mathrm{rel}}$.

Depending on the direction of the orientation field in the scattering region ($\mathbf{E}\uparrow\uparrow\mathbf{v}_{\mathrm{rel}}$ or $\mathbf{E}\uparrow\downarrow\mathbf{v}_{\mathrm{rel}}$) collisions on the head or on the tail of BC are preferred. The oriented wavefunction in the regular collision frame may be written as

$$\big|j,\pm\overline{m}_j,\overline{\Omega},E\big\rangle = \alpha(E)\big|j,\pm\overline{m}_j,\overline{\Omega},\epsilon_{\mathrm{u}}\big\rangle + \beta(E)\big|j,\pm\overline{m}_j,\overline{\Omega},-\epsilon_{\mathrm{u}}\big\rangle \tag{37}$$

or as

$$\big|j,\pm\overline{m}_j,\overline{\Omega},E\big\rangle = \alpha(E)\big|j,\pm\overline{m}_j,\overline{\Omega},\epsilon_{\mathrm{u}}\big\rangle - \beta(E)\big|j,\pm\overline{m}_j,\overline{\Omega},-\epsilon_{\mathrm{u}}\big\rangle. \tag{38}$$

Taking the limit for a high field E ($\alpha(E)=\beta(E)=\frac{1}{2}\sqrt{2}$) and subsequent substitution of these states in Eq. (3) leads to

$$\lim_{E\to\infty}\big|j,\pm\overline{m}_j,\overline{\Omega},E\big\rangle = \big|j,\pm\overline{m}_j,+\overline{\Omega}\big\rangle \tag{39}$$

or

$$\lim_{E\to\infty}\big|j,\pm\overline{m}_j,\overline{\Omega},E\big\rangle = \epsilon_{\mathrm{u}}\big|j,\pm\overline{m}_j,-\overline{\Omega}\big\rangle \tag{40}$$

The pairs of oriented wavefunctions that favor collisions onto the head (B) of BC in the regular frame of the (A–BC) CMS and onto the tail (C) in the regular frame of the (BC–A) CMS are represented by $\alpha(E)|j,\overline{m}_j,\overline{\Omega},\epsilon_{\mathrm{u}}\rangle - \beta(E)|j,\overline{m}_j,\overline{\Omega},-\epsilon_{\mathrm{u}}\rangle$ and $\alpha(E)|j,-\overline{m}_j,\overline{\Omega},\epsilon_{\mathrm{u}}\rangle + \beta(E)|j,-\overline{m}_j,\overline{\Omega},-\epsilon_{\mathrm{u}}\rangle$. The pair of wavefunctions $\alpha(E)|j,\overline{m}_j,\overline{\Omega},\epsilon_{\mathrm{u}}\rangle + \beta(E)|j,\overline{m}_j,\overline{\Omega},-\epsilon_{\mathrm{u}}\rangle$ and $\alpha(E)|j,-\overline{m}_j,\overline{\Omega},\epsilon_{\mathrm{u}}\rangle - \beta(E)|j,-\overline{m}_j,\overline{\Omega},-\epsilon_{\mathrm{u}}\rangle$ favor collisions onto the tail (C) of the molecule in the regular frame (A–BC) CMS and on the head in the regular frame of the (BC–A) CMS.

The orientation-dependent contribution

$$\frac{1}{2}(\mathrm{d}\sigma^{\mathrm{Head}}/\mathrm{d}\omega - \mathrm{d}\sigma^{\mathrm{Tail}}/\mathrm{d}\omega) \equiv \frac{\mathrm{d}}{\mathrm{d}\omega}\Delta\sigma_{j,m_j,\overline{\Omega},E\to j',m'_j,\overline{\Omega}',\epsilon'} \tag{41}$$

of the cross-section follows from Eqs. (8) and (9), upon insertion of the proper sign for $\beta(E)$. In the A–BC CMS one obtains

$$\frac{\mathrm{d}}{\mathrm{d}\omega}\Delta\sigma_{j,m_j,\overline{\Omega},E\to j',m'_j,\overline{\Omega}',\epsilon'} = \frac{-m_j}{\overline{m}_j}\alpha(E)\beta(E)\frac{1}{k^2}\left[f^{(\mathrm{A-BC})*}_{j,m_j,\overline{\Omega},\epsilon_{\mathrm{u}};j',m'_j,\overline{\Omega}',\epsilon'}(\hat{\mathbf{k}}')f^{(\mathrm{A-BC})}_{j,m_j,\overline{\Omega},-\epsilon_{\mathrm{u}};j',m'_j,\overline{\Omega}',\epsilon'}(\hat{\mathbf{k}}') + \mathrm{cc}\right]. \tag{42}$$

The complex conjugate is indicated by cc. Note that initial states with $m_j = 0$ cannot be oriented because of $m_j \cdot \Omega = 0$. When one compares Eq. (42) with Eq. (15) from [4], a sign mismatch appears when one assumes positive values for α and β conform the caption of Fig. 3 of [4]. In HIBRIDON, it is assumed that one works in the A–BC CMS, but the oriented wavefunction is taken with respect to the BC–A CMS similar to [1]. In the BC–A CMS, one gets

$$\frac{\mathrm{d}}{\mathrm{d}\omega}\Delta\sigma_{j,m_j,\overline{\Omega},E\to j',m'_j,\overline{\Omega}',\epsilon'} = \frac{m_j}{\overline{m}_j}\ \alpha(E)\beta(E)\frac{1}{k^2}\left[f^{(\mathrm{BC-A})*}_{j,m_j,\overline{\Omega},\epsilon_\mathrm{u};j',m'_j,\overline{\Omega}',\epsilon'}(\hat{\mathbf{k}}')f^{(\mathrm{BC-A})}_{j,m_j,\overline{\Omega},-\epsilon_\mathrm{u};j',m'_j,\overline{\Omega}',\epsilon'}(\hat{\mathbf{k}}') + \mathrm{cc}\right], \tag{43}$$

which yields the incorrect sign of S when one ignores the A–BC and BC–A dependence of the scattering amplitude that is based on the coupled T-matrix of Eq. (20). When taking this dependence into account by combining Eqs. (22), (42) and (43), identical outcome in the A–BC and the BC–A collision system results in $\frac{1}{2}(\mathrm{d}\sigma^{\mathrm{Head}}/\mathrm{d}\omega - \mathrm{d}\sigma^{\mathrm{Tail}}/\mathrm{d}\omega)$. This can offer an explanation for the discrepancy between the experimental and the theoretically calculated values of S for OH–Ar as presented in Section 3.

The expressions of Eqs. (42) and (43) both relate to the regular collision system. A switch from the regular to the reversed collision system also induces an additional sign change in Eqs. (42) and (43). The oriented states as defined in [1, Eqs. (8)–(11)] relate to the collision frame of the BC–A CMS. The m'_j summed orientational dependence of the integral A–BC collision cross-sections becomes

$$\frac{1}{2}(\sigma^{\mathrm{Head}} - \sigma^{\mathrm{Tail}}) = \int_{4\pi}\mathrm{d}\omega\sum_{m'_j}\frac{\mathrm{d}}{\mathrm{d}\omega}\Delta\sigma_{j,m_j,\overline{\Omega},E\to j',m'_j,\overline{\Omega}',\epsilon'}, \tag{44}$$

which, after defining $\Delta\sigma_{j,m_j,\overline{\Omega},E\to j,\overline{\Omega},\epsilon'} \equiv \sum_{m'_j}\Delta\sigma_{j,m_j,\overline{\Omega},E\to j',m'_j,\overline{\Omega}',\epsilon'}$ and making use of Eqs. (1.58) and (2.32) of [10] can be expressed as

$$\Delta\sigma_{j,m_j,\overline{\Omega},E\to j,\overline{\Omega},\epsilon'} = \frac{-2\pi}{k^2}\alpha(E)\beta(E)\sum_{J,l,l',l''\,(l+l''\mathrm{odd})}C^J_{l,l''}(j,\overline{m}_j)\times(-1)^{\frac{l-l''-1}{2}}\mathrm{Im}\left(T^{J,(\mathrm{A-BC})*}_{j',l',\overline{\Omega}',\epsilon';j,l,\overline{\Omega},\epsilon_\mathrm{u}}T^{J,(\mathrm{A-BC})}_{j',l',\overline{\Omega}',\epsilon';j,l'',\overline{\Omega},-\epsilon_\mathrm{u}}\right). \tag{45}$$

In experiments studying the orientational dependence of state-to-state rotational energy transfer of NO [1,5], a state with $j = \frac{1}{2}$ and $\overline{m}_j = \frac{1}{2}$ is selected. In this case, the summation over l and l'' restricts to $l = J \pm \frac{1}{2}$, $l'' = J \mp \frac{1}{2}$. From Eq. (26) it follows that

$$C^J_{J\pm\frac{1}{2},J\mp\frac{1}{2}}\left(\frac{1}{2},\frac{1}{2}\right) = \frac{1}{2}(2J+1). \tag{46}$$

Consequently, Eq. (45) can be reduced to

$$\Delta\sigma_{\frac{1}{2},m_j,\overline{\Omega},E\to j',\overline{\Omega}',\epsilon'} = \frac{-\pi}{k^2}\alpha(E)\beta(E)\sum_{J,l',\epsilon}(2J+1)\mathrm{Im}\left(T^{J,(\mathrm{A-BC})*}_{j',l',\overline{\Omega}',\epsilon';\frac{1}{2},J+\frac{1}{2},\overline{\Omega},\epsilon}T^{J,(\mathrm{A-BC})}_{j',l',\overline{\Omega}',\epsilon';\frac{1}{2},J-\frac{1}{2},\overline{\Omega},-\epsilon}\right). \tag{47}$$

This result can be transformed to the T-matrix $l + j \to J$ coupling scheme of van Leuken et al., using Eq. (6):

$$\Delta\sigma_{\frac{1}{2},m_j,\overline{\Omega},E\to j',\overline{\Omega}',\epsilon'} = \frac{\pi}{k^2}\alpha(E)\beta(E)\sum_{J,l',\epsilon}(2J+1)\mathrm{Im}\left(T^{J,(\mathrm{A-BC})*}_{l',j',\overline{\Omega}',\epsilon';J+\frac{1}{2},\frac{1}{2},\overline{\Omega},\epsilon}T^{J,(\mathrm{A-BC})}_{l',j',\overline{\Omega}',\epsilon';J-\frac{1}{2},\frac{1}{2},\overline{\Omega},-\epsilon}\right). \tag{48}$$

Comparison of Eq. (48) with Eq. (21) of [1] shows that for the theoretical results

$$(\sigma^{\mathrm{Head}} - \sigma^{\mathrm{Tail}})_{\mathrm{This\ work}} = (\sigma^{\mathrm{Head}} - \sigma^{\mathrm{Tail}})_{\mathrm{van\ Leuken}}. \tag{49}$$

This implies that the theoretical sign of S as obtained by van Leuken et al. [1] is correct.

The orientational dependence of OH in collisions has been studied for incoming oriented molecules with $\overline{\Omega} = j = \overline{m}_j = \frac{3}{2}$ [6,13,14]. In this case, the summation over l and l'' in Eq. (45) reduces to respectively: $l = J \pm \frac{3}{2}, l'' = J \mp \frac{3}{2}, l = J \pm \frac{1}{2}, l'' = J \mp \frac{1}{2}, l = J + 1 \pm \frac{1}{2}, l'' = J + 1 \mp \frac{1}{2}$ and $l = J - 1 \pm \frac{1}{2}, l'' = J - 1 \mp \frac{1}{2}$. Application of Eq. (26) for $\overline{m}_j = \frac{3}{2}$ yields for these special cases

$$C^J_{J\pm\frac{3}{2},J\mp\frac{3}{2}}\left(\frac{3}{2},\frac{3}{2}\right) = \frac{1}{8}\sqrt{\frac{(2J-1)(2J+3)}{2J(2J+2)}}(2J+1), \tag{50}$$

$$C^J_{J\pm\frac{1}{2},J\mp\frac{1}{2}}\left(\frac{3}{2},\frac{3}{2}\right) = \frac{3}{8}\sqrt{\frac{(2J-1)(2J+3)}{2J(2J+2)}}(2J+1), \tag{51}$$

$$C^{J}_{J+1\pm\frac{1}{2},J+1\mp\frac{1}{2}}\left(\frac{3}{2},\frac{3}{2}\right)=\frac{\sqrt{3}}{8}\frac{(2J-1)}{\sqrt{2J(2J+2)}}(2J+1) \tag{52}$$

and

$$C^{J}_{J-1\pm\frac{1}{2},J-1\mp\frac{1}{2}}\left(\frac{3}{2},\frac{3}{2}\right)=\frac{\sqrt{3}}{8}\frac{(2J+3)}{\sqrt{2J(2J+2)}}(2J+1). \tag{53}$$

Subsequent substitution of Eqs. (50)–(53) into Eq. (45) gives

$$\begin{aligned}\Delta\sigma_{\frac{3}{2},\overline{m}_j=\frac{3}{2},\overline{\Omega},E\to j',\overline{\Omega}',\epsilon'}=\frac{-\pi}{k^2}\alpha(E)\beta(E)\sum_{J,l',\epsilon}(2J+1)\mathrm{Im}\Bigg[&-\frac{1}{8}\sqrt{\frac{(2J-1)(2J+3)}{2J(2J+2)}}T^{J,(\mathrm{A-BC})*}_{j',l',\overline{\Omega}',\epsilon';\frac{3}{2},J+\frac{3}{2},\overline{\Omega},\epsilon}T^{J,(\mathrm{A-BC})}_{j',l',\overline{\Omega}',\epsilon';\frac{3}{2},J-\frac{3}{2},\overline{\Omega},-\epsilon}\\&+\frac{3}{8}\sqrt{\frac{(2J-1)(2J+3)}{2J(2J+2)}}T^{J,(\mathrm{A-BC})*}_{j',l',\overline{\Omega}',\epsilon';\frac{3}{2},J+\frac{1}{2},\overline{\Omega},\epsilon}T^{J,(\mathrm{A-BC})}_{j',l',\overline{\Omega}',\epsilon';\frac{3}{2},J-\frac{1}{2},\overline{\Omega},-\epsilon}\\&+\frac{\sqrt{3}}{8}\frac{(2J-1)}{\sqrt{2J(2J+2)}}T^{J,(\mathrm{A-BC})*}_{j',l',\overline{\Omega}',\epsilon';\frac{3}{2},J+\frac{3}{2},\overline{\Omega},\epsilon}T^{J,(\mathrm{A-BC})}_{j',l',\overline{\Omega}',\epsilon';\frac{3}{2},J+\frac{1}{2},\overline{\Omega},-\epsilon}\\&+\frac{\sqrt{3}}{8}\frac{(2J+3)}{\sqrt{2J(2J+2)}}T^{J,(\mathrm{A-BC})*}_{j',l',\overline{\Omega}',\epsilon';\frac{3}{2},J-\frac{1}{2},\overline{\Omega},\epsilon}T^{J,(\mathrm{A-BC})}_{j',l',\overline{\Omega}',\epsilon';\frac{3}{2},J-\frac{3}{2},\overline{\Omega},-\epsilon}\Bigg].\end{aligned} \tag{54}$$

Similar to the case of $\overline{m}_j=\frac{3}{2}$ (yielding Eqs. (50)–(60)) application of Eq. (26) for $\overline{m}_j=\frac{1}{2}$ gives

$$C^{J}_{J\pm\frac{3}{2},J\mp\frac{3}{2}}\left(\frac{3}{2},\frac{1}{2}\right)=-\frac{3}{8}\sqrt{\frac{(2J-1)(2J+3)}{2J(2J+2)}}(2J+1), \tag{55}$$

$$C^{J}_{J\pm\frac{1}{2},J\mp\frac{1}{2}}\left(\frac{3}{2},\frac{1}{2}\right)=-\frac{1}{8}\sqrt{\frac{(2J-1)(2J+3)}{2J(2J+2)}}(2J+1), \tag{56}$$

$$C^{J}_{J+1\pm\frac{1}{2},J+1\mp\frac{1}{2}}\left(\frac{3}{2},\frac{1}{2}\right)=\frac{\sqrt{3}}{8}\frac{(2J+3)}{\sqrt{2J(2J+2)}}(2J+1) \tag{57}$$

and

$$C^{J}_{J-1\pm\frac{1}{2},J-1\mp\frac{1}{2}}\left(\frac{3}{2},\frac{1}{2}\right)=\frac{\sqrt{3}}{8}\frac{(2J-1)}{\sqrt{2J(2J+2)}}(2J+1). \tag{58}$$

Subsequent substitution of Eqs. (55)–(58) into Eq. (45) for $\overline{m}_j=\frac{1}{2}$ results in

$$\begin{aligned}\Delta\sigma_{\frac{3}{2},\overline{m}_j=\frac{1}{2},\overline{\Omega},E\to j',\overline{\Omega}',\epsilon'}=\frac{-\pi}{k^2}\alpha(E)\beta(E)\sum_{J,l',\epsilon}(2J+1)\mathrm{Im}\Bigg[&\frac{3}{8}\sqrt{\frac{(2J-1)(2J+3)}{2J(2J+2)}}T^{J,(\mathrm{A-BC})*}_{j',l',\overline{\Omega}',\epsilon';\frac{3}{2},J+\frac{3}{2},\overline{\Omega},\epsilon}T^{J,(\mathrm{A-BC})}_{j',l',\overline{\Omega}',\epsilon';\frac{3}{2},J-\frac{3}{2},\overline{\Omega},-\epsilon}\\&-\frac{1}{8}\sqrt{\frac{(2J-1)(2J+3)}{2J(2J+2)}}T^{J,(\mathrm{A-BC})*}_{j',l',\overline{\Omega}',\epsilon';\frac{3}{2},J+\frac{1}{2},\overline{\Omega},\epsilon}T^{J,(\mathrm{A-BC})}_{j',l',\overline{\Omega}',\epsilon';\frac{3}{2},J-\frac{1}{2},\overline{\Omega},-\epsilon}\\&+\frac{\sqrt{3}}{8}\frac{(2J+3)}{\sqrt{2J(2J+2)}}T^{J,(\mathrm{A-BC})*}_{j',l',\overline{\Omega}',\epsilon';\frac{3}{2},J+\frac{3}{2},\overline{\Omega},\epsilon}T^{J,(\mathrm{A-BC})}_{j',l',\overline{\Omega}',\epsilon';\frac{3}{2},J+\frac{1}{2},\overline{\Omega},-\epsilon}\\&+\frac{\sqrt{3}}{8}\frac{(2J-1)}{\sqrt{2J(2J+2)}}T^{J,(\mathrm{A-BC})*}_{j',l',\overline{\Omega}',\epsilon';\frac{3}{2},J-\frac{1}{2},\overline{\Omega},\epsilon}T^{J,(\mathrm{A-BC})}_{j',l',\overline{\Omega}',\epsilon';\frac{3}{2},J-\frac{3}{2},\overline{\Omega},-\epsilon}\Bigg].\end{aligned} \tag{59}$$

The equations above describe a recipe to calculate $\frac{1}{2}(\sigma^{\mathrm{Head}}-\sigma^{\mathrm{Tail}})$, which presents the numerator of S as defined in Eq. (1). Its denominator $\frac{1}{2}(\sigma^{\mathrm{Head}}+\sigma^{\mathrm{Tail}})$ can be calculated using Eq. (42) as

$$\frac{1}{2}(\sigma^{\mathrm{Head}}+\sigma^{\mathrm{Tail}})=\alpha^2(E)\sigma_{j,m_j,\overline{\Omega},\epsilon_{\mathrm{u}}\to j',\overline{\Omega}',\epsilon'}+\beta^2(E)\sigma_{j,m_j,\overline{\Omega},-\epsilon_{\mathrm{u}}\to j',\overline{\Omega}',\epsilon'}. \tag{60}$$

In the case of $j=\frac{1}{2}$ and $j=\frac{3}{2}$, Eqs. (28), (32) and (36) provide a recipe for calculation of $\sigma_{j,m_j,\overline{\Omega},\epsilon\to j',\overline{\Omega}',\epsilon'}$. Substitution of $\sigma_{j,m_j,\overline{\Omega},\epsilon\to j',\overline{\Omega}',\epsilon'}$ in Eq. (60) yields S.

5. Re-evaluation of the experimental sign of the steric asymmetry

Except for the very first tentative observations [1], the experimentally obtained values of S for NO–Ar confirmed the theoretical predictions [3–5]. Both calculated and experimental values of S for high j' are in disagreement with a ball and stick model. The present (close-coupling) HIBRIDON calculations for OH–Ar result in a sign for S that is improper compared to earlier measurements and which is also opposite to the ball and stick model. As argued in Section 4.3 below Eq. (43), this can be explained by the fact that the oriented wavefunction in HIBRIDON carries an actual orientation that is opposite to the denoted one. The assumption that the ball and stick model is correct for OH–Ar, implies that the sign of S for HIBRIDON calculations (probably also for NO–Ar) has to be reversed. This raises the question whether the experimental results for NO–Ar have to be revised, possibly due to errors in the experimental procedure. Therefore the experimental sign of S has been reinvestigated to explore this possibility. As a first step, the direction of the orientation field in relation to the data acquisition and control software has been checked. Using a voltmeter, the voltage on the rods of the orientation field was measured and found to be in correspondence with the assumed value in the software.

To exclude the possibility that the previous experiments had been carried out incorrectly, the steric asymmetry has been remeasured for NO–He (at $E_{\mathrm{tr}} = 514\ \mathrm{cm}^{-1}$) for a transition to the final state $j' = 4.5$, $\overline{\Omega}' = \frac{1}{2}$, $\epsilon' = -1$. This remeasurement has been carried out under similar conditions as in earlier measurements for NO–Ar and NO–He [5,16], but with a more powerful laser and a new data acquisition program. The earlier measurements on NO–Ar and NO–He showed that NO–He yields the same sign for S as NO–Ar [16]. In both measurements laser induced fluorescence from the $A\,^2\Sigma^+(v = 0)$ state was used to determine the total number of molecules scattered into the $j' = 4\frac{1}{2}, \overline{\Omega}' = \frac{1}{2}, \epsilon' = -1$ level of the vibrational ground state.

The laser system that was used in earlier work has been replaced by a more powerful excimer pumped dye laser system (Lambda Physik EMG 201/FL 3002) equipped with a frequency doubling unit to generate the tunable $\lambda = 226$ nm (output 1.5 mJ/pulse). This new laser system required a new timing and control system for which new software was developed. New software for data acquisition was also developed and the orientation voltages were tested once again and found to be correct. A value of $S = 0.28 \pm 0.02$ was obtained earlier by de Lange et al. in the case described above [5]. Our remeasurement yielded a value of $S = 0.39 \pm 0.15$ which confirms the correctness of de Lange's NO–Ar data collection procedure.

The next step in our re-evaluation was to look for physical explanations for an orientation of the NO molecule in the scattering region, opposite to the expected orientation. Opposite orientation of the NO molecule would change the sign of the theoretical predicted S, so N-end collisions are preferred for excitation to high rotational states. If a molecule in

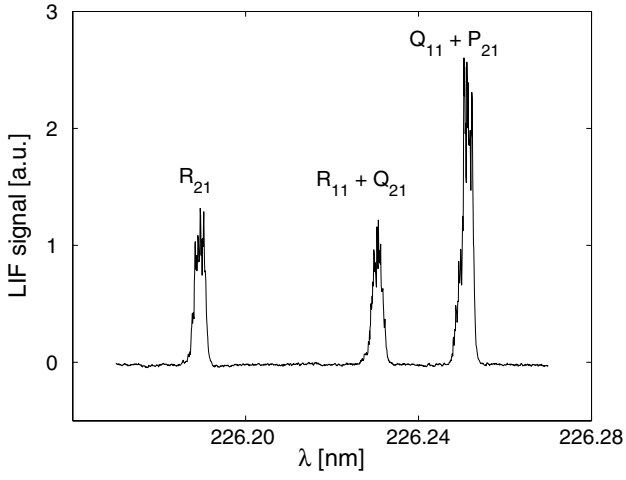

Fig. 5. LIF excitation spectrum of $A\,^2\Sigma^+(v = 0) \leftarrow X\,^2\Pi_{1/2}(v = 0)$ transition of the hexapole state selected NO beam, taken under the same conditions at which S was remeasured. The spectrum is somewhat saturated and an orientation field of $E \approx 16$ kV/cm is applied that is expected to induce about 25% mixing with the lower component ($\epsilon = 1$) of the Λ-doublet [9]. The R_{21} and the Q_{11} originate from the hexapole selected upper $\epsilon = -1$ component of the $j = \frac{1}{2}$ Λ-doublet. The R_{11}/Q_{21} transition, that originates from the lower component of the Λ-doublet is due to the mixing of the Λ-doublet, caused by the orientation field. When the field is switched off, the center peak (R_{11}/Q_{21} branch) disappears, while the other peaks remain. In absence of saturation and at equal population of both components of the Λ-doublet component, LIF intensities will be proportional to Hönl-London factors giving a ratio of $R_{21} : Q_{11} : R_{11}/Q_{21}$ as 1 : 2 : 3. Clearly the spectrum shows approximately 25% mixing in the lower Λ-doublet component. This means that the NO molecules in the scattering region are in a low field seeking state. A Majorana flop is excluded.

a low field seeking state undergoes a rapid change of the electric field along its path, this can result in a sudden change of the low field seeking state into that of a high field seeking state. This phenomenon is known under the name Majorana flop [27,29]. When such an effect would occur in our setup the sign of the experimental reported S would reverse and agree with the proper sign (in accordance to the ball and stick model) of the theoretical S, as argued in this work. The presence of an orientational Majorana flop has been investigated experimentally by examining the LIF spectrum of the $A^2\Sigma^+(v=0) \leftarrow X^2\Pi_{\frac{1}{2}}(v=0)$, under the same conditions at which S was remeasured (Fig. 5). When no orientation field is present, one expects to see only two peaks for the hexapole state selected beam, the R_{21} and the Q_{11} branch. If a field is applied, mixing of Λ-doublet as defined in Eq. (8) will take place and the peak of the R_{11}/Q_{21} branches appears. Peaks belonging to the lower and high field seeking Λ-doublet state will occur and grow with increasing orientation field strength. This effect is seen, but in the case of a Majorana flop, the high field seeking R_{11}/Q_{21} peak ought to dominate the spectrum. In the experiment it does not. The experiment shows that it is the low field seeking component of the Λ-doublet that is present in the collision region. This component orients with its negative end towards the negative electrode of the orientation field rods.

6. Discussion and concluding remarks

Theoretical and experimental results for S in NO–Ar collisions showed an O-end preference for transitions to high final rotational states [1,5]. From a (classical) ball and stick model one would expect the N-end to be preferred, as the torque that can be applied on the N-end is larger. For collisions of the less homo-nuclear OH molecule with Ar, the simple ball and stick model does apply. The H-end is preferred for high rotational states in both experiments and theoretical results [6]. To our knowledge, there is no satisfactory answer to the question why S for OH–Ar does behave as expected, while for NO–Ar it behaves oppositely. Application of a newly developed semi-quantum mechanical model [17] yields reasonable values for the amplitude of S, but gives a sign for NO–Ar that is opposite to experimental one. For OH–Ar it yields the proper sign, so its result can in both cases be explained by the ball and stick model. The present quantum mechanical (HIBRIDON) calculations on collisions of OH–Ar (this work) yield an opposite sign of S: a preference for O-end collisions for transitions to high rotational states. Although this does not correspond to the ball and stick model, it is consonant with the NO–Ar results.

Assuming that the OH–Ar measurements are correct (as they can easily be understood), then HIBRIDON calculations yield the wrong sign for S. A sign error in the expressions of van Leuken [1] for collisions involving NO is excluded, as can be concluded from the outcome of Section 4.3. A feasible possibility is an error in the implementation of HIBRIDON. In HIBRIDON it is assumed that one works in the A-BC CM system, while the oriented wavefunctions are taken in respect to the BC-A CMS. This inconsistency induces a switch of the sign of S. Implementation problems in the adapted version of MOLSCAT could not be explored, as its originator Prof. J. Snijders sadly passed away in 2003 and no documentation was left.

When for NO–Ar the sign of quantum mechanical calculations has to switch as well, all theoretical results are consonant with the ball and stick model. The experimental results for NO–Ar have been checked and were found to be opposite to the ball and stick model. Experimentally, it has been shown that molecules in the collision region are in the low field seeking state. The negative end is assumed to correspond to the head (N-end) and the positive end to the tail (O-end) of the NO molecule. Under this assumption, the actually observed steric asymmetry S is given by:

$$S = \frac{\sigma^- - \sigma^+}{\sigma^- + \sigma^+}. \tag{61}$$

The cross-sections σ^- and σ^+, respectively, indicate the cases in which the negative and the positive end of the molecule preferentially point towards the incoming atom. If the sign of the NO($v=0$, $X^2\Pi$) dipole moment would be reversed, N^+O^- instead of N^-O^+, the experimental sign of S would be in agreement with the ball and stick model.

The absolute value of the small electric dipole of NO($v=0$, $X^2\Pi$) has been measured with high precision (0.1574 ± 0.014 D) by Hoy et al. [31], whose result is in reasonable agreement with the ab initio value: 0.1732 D [32]. Although the absolute value of the NO dipole moment is well known, even the highest precision experiments cannot determine the sign of the NO dipole moment, i.e., N^-O^+ or N^+O^- [33]. In past experiments [33–36], the assumed sign of the NO($v=0$, $X^2\Pi$) dipole is based on the outcome of large series of ab initio calculations that all reported N^-O^+ [32,37–40]. Taking into account recent experiments by Matsiev and coworkers [41] and predictions by Drabbels and Wodtke [33], a flip of the sign of the dipole moment seems not to be feasible.

Except for the sign of S, there is a good quantitative agreement regarding the amplitude of S between NO–Ar collision experiments and their theory. Thus the possibility that the CEPA and CCSD(T) PESs are not accurate enough, can be excluded. Besides this, the observed excitation spectrum of the bound Ar–NO($v=0$, $X^2\Pi$) van der Waals

complex has been found to agree very well with its theoretical prediction based on the CEPA and on the CCSD(T) PESs [30]. This does not exclude that the labels for the N- and the O-end in the PESs might be wrong. However, it is very unlikely to assume that the heavier O-end extends further from the center-of-mass than the N-end.

A very unlikely option is that van Beek et al. made an experimental error and that also their previous theoretical calculations carry the wrong sign for S [6]. In this case both NO–Ar and OH–Ar behave oppositely to the ball and stick model. The previous theoretical calculations [1,3,4] for NO–Ar and the present calculated values of Table 1 for OH–Ar are found to agree with experiments.

The last option is that only the present HIBRIDON calculations (as listed in Table 1) are erroneous, due to errors outside the actual program (e.g. input parameters). Previous calculations for both NO–Ar and OH–Ar could not carry these errors, which would explain the agreement between the theoretical and experimental sign for both cases. This cannot explain the opposite behavior of S for NO–Ar and OH–Ar, where OH–Ar does and NO–Ar does not behave as expected from a ball and stick model. Although this last option can never be excluded completely, no errors could be found.

Clearly, to render a satisfactory explanation for the sign issue concerning the steric asymmetry and to resolve the disagreement between the experimental and predicted theoretical values for S, further work is required.

Acknowledgements

The authors express their gratitude to Prof. Ad van der Avoird for his support and interest and to Dr. J. Bulthuis, Dr. M.H.M. Janssen, Dr. C.A. Taatjes and Prof. A.M. Wodtke for helpful contributions and discussions. The authors are also very grateful to Prof. A.W. Kleyn for his contribution of an excimer/dye laser system. The Netherlands Organization for Scientific Research (NWO) is gratefully acknowledged for financial support through CW and FOM. J. K*error*os acknowledges financial support from the European Research Training Network THEONET II.

References

[1] J.J. van Leuken, J. Bulthuis, S. Stolte, J.G. Snijders, Chem. Phys. Lett. 260 (1996) 595.
[2] M.H. Alexander, P. Andresen, R. Bacis, R. Bersohn, F.J. Comes, P.J. Dagdigian, R.N. Dixon, R.W. Field, G.W. Glynn, K.H. Gericke, E.R. Grant, B.J. Howard, J.R. Huber, D.S. King, J.L. Kinsey, K. Kleinermanns, K. Kuchitsu, A.C. Luntz, A.J. McCaffery, B. Pouilly, H. Reisler, S. Rosenwaks, E.W. Rothe, M. Shapiro, J.P. Simons, R. Vasudev, J.R. Wiesenfeld, C. Wittig, R.N. Zare, J. Chem. Phys. 89 (1988) 1749.
[3] M.H. Alexander, Faraday Discuss. Chem. Soc. 113 (1999) 437.
[4] M.H. Alexander, S. Stolte, J. Chem. Phys. 112 (2000) 8017.
[5] M.J.L. de Lange, M. Drabbels, P.T. Griffiths, J. Bulthuis, J.G. Snijders, Chem. Phys. Lett. 313 (1999) 491.
[6] M.C. van Beek, J.J. ter Meulen, M.H. Alexander, J. Chem. Phys 113 (2000) 637.
[7] HIBRIDON is a package of programs for the time independent quantum treatment of inelastic collisions written by M.H. Alexander, D.E. Manolopoulos, H.J. Werner, B. Follmeg, with contributions by P.F. Vohralik, D. Lemoine, G. Corey, R. Gordon, B. Johnson, T. Orlikowski, A. Berning, A. Degli-Esposti, C. Rist, P. Dagdigian, B. Pouilly, G. van der Sanden, M. Yang, F. de Weerd, S. Gregurick. More information and a copy of the code can be obtained from http://www.chem.umd.edu/physical/alexander/hibridon/.
[8] J. Klos, G. Chalasinski, M.T. Berry, R.A. Kendall, R. Burcl, M. Szczesniak, S.M. Cybulski, J. Chem. Phys. 112 (2000) 4952.
[9] M.J.L. de Lange, J.J. van Leuken, M. Drabbels, J. Bulthuis, J.G. Snijders, S. Stolte, Chem. Phys. Lett. 294 (1998) 332.
[10] R.N. Zare, Angular Momentum: Understanding Spatial Aspects in Chemistry and Physics, Wiley, New York, 1988.
[11] A.M. Arthurs, A. Dalgarno, Proc. R. Soc. Lond. Ser. A 256 (1960) 540.
[12] M.H. Alexander, J. Chem. Phys. 76 (1982) 5974.
[13] K. Schreel, J.J. ter Meulen, J. Chem. Phys. 101 (1997) 7639.
[14] M.C. van Beek, G. Berden, H.L. Bethlem, J.J. ter Meulen, Phys. Rev. Lett. 86 (2001) 4001.
[15] M.C. van Beek, J.J. ter Meulen, J. Chem. Phys. 115 (2001) 1843.
[16] M.J.L. de Lange, Ph.D. Thesis, Vrije Universiteit, Amsterdam, 2003.
[17] A. Gijsbertsen et al., manuscript in preparation.
[18] A.D. Esposti, H.-J. Werner, J. Chem. Phys. 93 (1990) 3351.
[19] M.H. Alexander, J. Chem. Phys. 99 (1993) 7725.
[20] M.H. Alexander, J. Chem. Phys. 111 (1999) 7426.
[21] J.M. Hutson, S. Green, MOLSCAT computer code, version 14 (1994), distributed by Collaborative Computational Project No. 6 of the Engineering and Physical Sciences Research Council, UK.
[22] M.C. van Beek, J.J. ter Meulen, M.H. Alexander, J. Chem. Phys. 113 (2000) 628.
[23] M.S. Child, Molecular Collision Theory, Dover Mineola, NY, 1996.
[24] R.D. Levine, R.B. Bernstein, Molecular Reaction Dynamics and Chemical Reactivity, Oxford University Press, Oxford, 1987.
[25] S. Stolte, J. Reuss, Chapter 5, in: R.B. Bernstein (Ed.), Atom–Molecule Collision Theory, Plenum Press, New York, 1979, p. 201.
[26] H.J. Loesch, Annu. Rev. Phys. Chem. 46 (1995) 555.

[27] S. Stolte, in: G. Scoles (Ed.), Atomic and Molecular Beams Methods, vol. 14, Oxford University Press, New York/Oxford, 1988, p. 631 (Chapter 25).
[28] D.H. Parker, H. Jalink, S. Stolte, J. Phys. Chem. 91 (1987) 5427.
[29] C. Maltz, N.O. Weinstein, D.R. Herschbach, Mol. Phys. 24 (1972) 133.
[30] Y. Kim, J. Fleniken, H. Meyer, M.H. Alexander, P.J. Dagdigian, J. Chem. Phys. 113 (2000) 73.
[31] A.R. Hoy, J.W.C. Jons, A.R.W. McKellar, Can. J. Phys. 53 (1975) 2029.
[32] S.R. Langhoff, C.W. Bauschlicher, H. Partridge, Chem. Phys. Lett. 223 (1994) 416.
[33] M. Drabbels, A.M. Wodtke, Chem. Phys. Lett. 256 (1996) 8.
[34] K.W. Holtzclaw, W.T. Rawlins, B.D. Green, J. Quant. Spectrosc. RA. 55 (1996) 481.
[35] M. Drabbels, A.M. Wodtke, J. Chem. Phys. 106 (1997) 3024.
[36] W.T. Rawlins, J.C. Person, M.E. Fraser, S.M. Miller, W.A.M. Blumberg, J. Chem. Phys. 109 (1998) 3409.
[37] S. Green, Chem. Phys. Lett. 23 (1973) 115.
[38] F.P. Billingsley, J. Chem. Phys. 62 (1975) 864;
J. Chem. Phys. 63 (1975) 2267.
[39] R. de Vivie, S.D. Peyerimhoff, J. Chem. Phys. 89 (1988) 3028.
[40] R. Sayós, R. Valero, J.M. Anglada, M. González, J. Chem. Phys. 112 (2000) 6608.
[41] D. Matsiev, J. Chen, M. Murphy, A.M. Wodtke, J. Chem. Phys. 118 (2003) 9477.